GPS Solutions (2023) 27:61
https://doi.org/10.1007/s10291-023-01402-y

ORIGINAL ARTICLE

An investigation of PPP time transfer via BDS-3 PPP-B2b service

Yulong Ge[1] · Xinyun Cao[2] · Daqian Lyu[3] · Zaimin He[4] · Fei Ye[5] · Gongwei Xiao[4] · Fei Shen[2]

Received: 27 May 2022 / Accepted: 11 January 2023 / Published online: 26 January 2023

Abstract
Since 2020, China's Beidou has begun to provide an initial real-time precise point positioning (PPP) service via B2b signals for the Asia–Pacific region. It is expected to be used to achieve centimeter-level positioning and also brings opportunities for real-time time transfer. We collected 29 days of experimental data and compared it with the Centre National d'Etudes Spatiales (CNES) real-time products. The quality of the satellite's orbit and clock was analyzed first. Then, time transfer based on BDS-3, GPS, and BDS-3/GPS PPP was investigated. The results showed that the GPS PPP with the PPP-B2b is not recommended. The time transfer based on BDS-3 PPP using the PPP-B2a is feasible and achieves a 0.30 ns level. Importantly, the reliability of time transfer using the PPP-B2b outperforms that of PPP using CNES products due to the problem of unstable internet communication. Furthermore, compared to BDS-3-only, the precision of time transfer based on BDS-3/GPS PPP was not improved significantly.

Keywords Time transfer · BDS-3/GPS · Real-time PPP · PPP-B2b

Introduction

The BDS-3 in China has been providing all-weather, continuous PNT services for the world since July 31, 2020 (Lu et al. 2020; Yang et al. 2019, 2020). Nowadays, there are 24 MEO, 3 GEO, and 3 IGSO that make up the BDS-3 constellation. Compared to BDS-2, in terms of frequency, BDS-3 has added three new signals, B1C, B2b, and B2a, in addition to continuing to retain the B1I/B3I signals (CSNO 2019, 2020a). In addition, the quality of the signals outperforms that of BDS-2, especially since the signals of BDS-3 no longer have the problem of satellite-induced code bias (Zhang et al. 2017a; b). Furthermore, a hydrogen clock was installed on BDS-3, which provides better precision and a more stable frequency standard for navigation signals (Wu et al. 2018).

A large number of scholars have begun to study the BDS-3 in various fields, such as precise orbit determination (Duan et al. 2019; Li et al. 2018b, c), satellite clock offset estimation (Cao et al. 2022; Yang et al. 2021; Zeng et al. 2020), tropospheric delay estimation (Ge et al. 2021b), precise positioning (Jiao et al. 2020; Li et al. 2020; Shi et al. 2020, 2021) and time transfer (Ge et al. 2021a; Guang et al. 2020; Xiao et al. 2021; Zhang et al. 2019). For precise applications, two representative technologies are Real-time Kinematic (RTK) and PPP (Malys and Jensen 1990; Shi et al. 2020; Zumberge et al. 1997). IGS has provided RTS for PPP since 2013, for the needs of users (Montenbruck et al. 2017). Wang et al. (2019) studied the BDS-2 PPP using real-time products released from CNES and concluded that its positioning accuracy reaches to several decimeters due to the poor quality of the BDS-2 real-time products. Zhao et al. (2020) investigated the real-time GNSS PPP with CNES products in kinematic mode and presented the positioning accuracy of about 3.2, 2.9, and 6.0 cm at ENU direction, respectively.

✉ Xinyun Cao
xycao@njnu.edu.cn

1 School of Marine Science and Engineering, Nanjing Normal University, Nanjing 210023, China

2 School of Geography, Nanjing Normal University, Nanjing 210023, China

3 College of Electronic Engineering, National University of Defense Technology, Hefei 230037, China

4 School of Communication and Information Engineering, Xi'an University of Posts and Telecommunications, Xi'an 710121, China

5 State Key Laboratory of Geodesy and Earth's Dynamics, Innovation Academy for Precision Measurement Science and Technology, CAS, Wuhan 430077, China

In addition to positioning, timing is also one of the important service capabilities of BeiDou satellites (CSNO 2019). Nowadays, the PPP technique is widely applied in the time community. Subsequently, Li et al. (2018a) released sub-nanosecond level time transfer using IGS real-time products. Furthermore, Ge et al. (2021b) analyzed the BDS-3 real-time PPP time transfer and reached the sub-nanosecond level. But real-time PPP using IGS RTS products is difficult to guarantee reliability and is susceptible to network outages that cause PPP to re-converge or even become unavailable. For this background, BDS-3 can now provide PPP-B2b service via B2b signals to Asia by three BDS-3 GEO satellites (CSNO 2020a, b). PPP with PPP-B2b service in precise positioning was analyzed by some researchers (Liu et al. 2022; Tao et al. 2021; Xu et al. 2021; Yang et al. 2022). Little has been published on time transfer with the PPP-B2b; hence, the performance of BDS-3, GPS, and BDS-3/GPS PPP time transfer with the PPP-B2b service will be investigated in this contribution.

The method of recovery of precise clock offset and orbit will be presented first, followed by PPP time transfer with the PPP-B2b. The quality of real-time products will then be assessed and analyzed. Next, the experimental dataset and the processing strategies are described in detail. Following that is the investigation and validation of PPP time transfer with the PPP-B2b correction. Finally, the findings are concluded.

Methodology

This part introduces the recovery of precise orbit and clock using broadcast ephemeris and PPP-B2b correction. Then, the PPP time transfer method is presented and the processing of PPP time transfer with the PPP-B2b service is illustrated in detail.

Precise orbit and clock offset recovered from PPP-B2b service

Precise orbit can consist of broadcast ephemeris and PPP-B2b correction (Xu et al. 2021), which is expressed as:

$$\begin{cases} \mathbf{X} = \mathbf{X}_{\text{brd}} + (\mathbf{e}_r, \mathbf{e}_a, \mathbf{e}_c) \cdot \Delta\mathbf{C} \\ \Delta\mathbf{C} = [\delta C_r, \delta C_a, \delta C_c] \\ \boldsymbol{e}_r = \dfrac{\boldsymbol{r}}{|\boldsymbol{r}|} \\ \boldsymbol{e}_c = \dfrac{\boldsymbol{r} \times \dot{\boldsymbol{r}}}{|\boldsymbol{r} \times \dot{\boldsymbol{r}}|} \\ \boldsymbol{e}_a = \boldsymbol{e}_c \times \boldsymbol{e}_r \end{cases} \tag{1}$$

where $\mathbf{X}$ is the vector of precise orbit in meters; $(\mathbf{e}_r, \mathbf{e}_a, \mathbf{e}_c)$ indicates the transformation matrix in RAC direction; $\mathbf{X}_{\text{brd}}$ is the orbits calculated from broadcast ephemeris; $\Delta\mathbf{C}$ is the PPP-B2b correction at RAC direction; $\dot{\boldsymbol{r}}$ and $\boldsymbol{r}$ are the vector of satellite velocity and position in the ECEF. Note that the PPP-B2b service provides the satellite APC position of the B3 signal for BDS-3; hence, for B1I/B3I IF combination or another PPP model, the APC satellite position needs to be corrected to the corresponding frequency combination (Tao et al. 2021). For GPS, the APC of the position of the satellite refers to L1/L2 IF combination.

The precise satellite clock is recovered by the broadcast ephemeris clock and the corrections from the PPP-B2b service as:

$$t = t_{brd} - \frac{\Delta t}{c} \tag{2}$$

where t_{brd} indicates satellite clock in broadcast ephemeris; t illustrates the precise satellite clock offsets; Δt is the correction in the PPP-B2b service. c is the speed of light. Note further that the OSB corrections from the PPP-B2b service need to be modified to the corresponding pseudorange observations.

PPP Time transfer

DF IF combination is usually employed for PPP (Tu et al. 2019). The DF IF combination is usually written as:

$$p^s_{r,IF_{ij}} = \boldsymbol{\mu}^s_r \cdot \Delta\mathbf{x} + cdt_{r,IF_{ij}} + m^s_{r,w} \cdot Z_w + \xi^s_{r,IF_{ij}} \tag{3}$$

$$l^s_{r,IF_{ij}} = \boldsymbol{\mu}^s_r \cdot \Delta\mathbf{x} + cdt_{r,IF_{ij}} + m^s_{r,w} \cdot Z_w + N^s_{r,IF_{ij}} + \psi^s_{r,IF_{ij}} \tag{4}$$

$$\begin{cases} cdt_{r,IF_{ij}} = cdt_r + cd_{r,IF_{ij}} \\ d_{r,IF_{ij}} = \alpha_{ij} d_{r,i} + \beta_{ij} d_{r,j} \\ \alpha_{ij} = \dfrac{f_i^2}{f_i^2 - f_j^2}; \beta_{ij} = -\dfrac{f_j^2}{f_i^2 - f_j^2}; i \neq j \end{cases} \tag{5}$$

where $p^s_{r,IF_{ij}}$ and $l^s_{r,IF_{ij}}$ are the OMC values for IF pseudorange and carrier phase observations; Here, s and r indicate the satellites and receiver; $\Delta\mathbf{x}$ illustrates the coordinate increment;$\boldsymbol{\mu}^s_r$ is the vector of coefficient for coordinates; i and j are the different frequencies. For BDS-3 and GPS satellites, B1I/B3I and L1/L2 combinations are selected to realized PPP time transfer; $d_{r,i}$ indicates the hardware delay for frequency i at receiver end; f_i represents frequency i; dt_r is the receiver clock offset; $dt_{r,IF_{ij}}$ presents the receiver clock offset for i and j frequency IF combination (IF_{ij}) including the hardware delay; $d_{r,IF_{ij}}$ indicates the hardware delay for i and

j frequency IF combination; Z_w is the tropospheric ZWD; $m^s_{r,w}$ demonstrates the wet mapping function; $N^s_{r,IF_{ij}}$ is the float IF ambiguity; $\psi^s_{r,IFij}$ and $\xi^s_{r,IF_{ij}}$ are the noise. In addition, based on elevation-dependent weighting used in our work, the precision of orbit and clock calculated from the PPP-B2b correction also need to be considered. The weight **W** can be expressed as

$$\begin{cases} \mathbf{W} = diag(\sigma_1^{-2}, \sigma_2^{-2}, \sigma_3^{-2}, \cdots, \sigma_m^{-2}) \\ \sigma^2 = FR_r(a_\sigma^2 + b_\sigma^2 / \sin E^2) + \sigma_{eph}^2 \end{cases} \tag{6}$$

where F is the satellite system error factor; R_r indicates code/carrier phase error ratio; a_σ and b_σ^2 are carrier-phase error factors a and b (m); E illustrates elevation angle; σ_{eph} is the URA from the PPP-B2b service; m is the number of satellites.

Unlike final products from MGEX or real-time multi-GNSS products from IGS RTS, the reference for the BDS-3 satellite clock is the BDT in the PPP-B2b service, which is more stable and continuous. However, the reference of the GPS satellite clock is not aligned to the same time reference; fortunately, this phenomenon does not affect the performance of time transfer (Tao et al. 2021; Yang et al. 2022). The receiver clock offset $cdt_{r,IF_{ij}}$, estimated from the PPP model using BDS-3, consists of the difference between BDT and the local time, and the hardware delay. Generally, the hardware delay is calibrated in advance. The difference D_u between local time and BDT can then be described as

$$D_u = T_{local} - \mathrm{BDT} \tag{7}$$

where u indicates the user; T_{local} demonstrates the local time of the users.

For two different places, the difference ΔT will be expressed as

$$\begin{aligned} \Delta \mathrm{T} &= D_1 - D_2 \\ &= T_1 - \mathrm{BDT} - (T_2 - \mathrm{BDT}) \\ &= T_1 - T_2 \end{aligned} \tag{8}$$

where T_1 and T_2 are the local time of different users.

For each station, receiving the BDS-3 or GPS pseudorange and phase observation and 3 GEO satellite signals for decoding PPP-B2b corrections. Based on BDS-3 CNAV1 and GPS LNAV broadcast ephemeris and decoded the PPP-B2b correction, precise orbit and clock offset are then recovered. Note that the OSB correction will be corrected directly for pseudorange at each frequency. Next, the time difference between BDT and the local time will be estimated directly by using the corresponding PPP model. Finally, the time transfer solutions can be obtained directly using Eq. (8).

Assessment of precise products recovered from the PPP-B2b

The quality of orbit and clock determines PPP time transfer performance directly. 29 days, from DOY 122 to 131, 2022 and from DOY 144 to 162, 2022, precise products recovered from the PPP-B2b are compared and evaluated with WUM final products released from Wuhan University, China. The RMSs of BDS-3 and GPS orbit errors for the CNES real-time products and PPP-B2b are presented in Figs. 1 and 2 and listed in Table 1, respectively, at RAC directly with respect to WUM products. Overall, the GPS orbit errors at the radial direction for the PPP-B2b are approximately

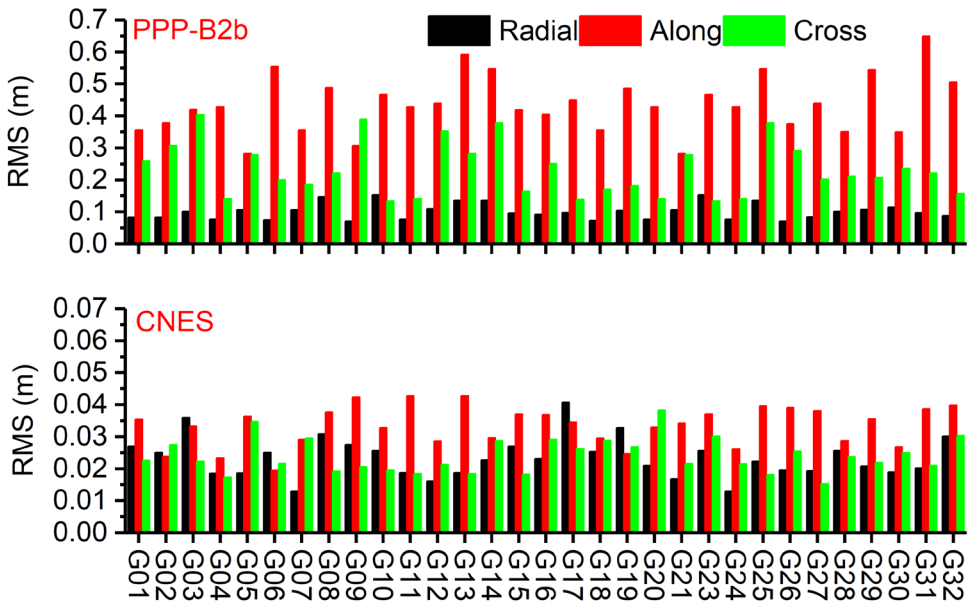

Fig. 1 Orbits errors of GPS satellites for the CNES's real-time products (Bottom) and PPP-B2b (Top) in the RAC direction

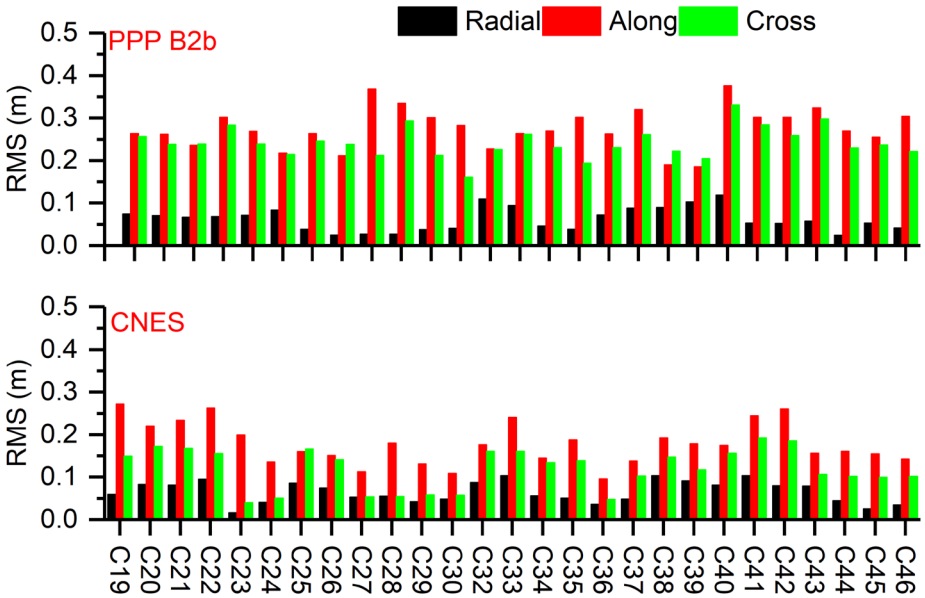

Fig. 2 Orbits errors of BDS-3 in the CNES real-time products (Bottom) and PPP-B2b (Top) in the RAC direction

Table 1 Mean RMS values of GPS or BDS-3 orbit errors in the PPP-B2b and the CNES real-time products with respect to WUM final products

	PPP-B2b (m)			CNES's real-time products (m)		
	R	A	C	R	A	C
GPS	0.10	0.43	0.23	0.02	0.03	0.02
BDS-3	0.07	0.27	0.23	0.07	0.18	0.12

0.1 m, while the orbit errors are relatively large at along and cross-directions. The mean RMS values in the RAC vector are about (0.10, 0.43, 0.23) m. For CNES real-time GPS products, the orbit errors agree with each other at the RAC direction; the mean RMS values in the RAC vector are approximately (0.02, 0.03, 0.02) m. The precision of GPS orbit in PPP-B2b is obviously worse than that of CNES, especially in the cross and along components. The reason is that a global network is employed by CNES, while only a regional network is applied for GPS in the PPP-B2b (Tao et al. 2021). For BDS-3 satellites, an interesting finding is that the precision of BDS-3 orbit at along component is better than that of GPS in the PPP-B2b. That may be because BDS-3 is equipped with ISL terminals, which provide additional observations (Tang et al. 2018). The average RMS values for BDS-3 with PPP-B2b are about (0.07, 0.27, 0.23) m at RAC direction. For BDS-3 in CNES products, the precision of BDS-3 orbit is worse than that of GPS with (0.07, 0.18, 0.12) m at RAC direction, which may be due to the poor distribution of BDS-3 tracking station as compared to GPS.

To further evaluate the satellite clock offset recovered from the PPP-B2b, the double-difference (DD) method was employed by using WUM final clock products as the reference (Montenbruck et al. 2014), with G01 and C38 selected as references. The STD values of DD GPS and BDS-3 satellite clock recovered from CNES and PPP-B2b are displayed in Figs. 3 and 4. For the GPS constellation, the STD values of PPP-B2b are about 2 times larger than that of CNES. The average STD values of GPS satellite clocks are about 0.13 ns and 0.06 ns for PPP-B2b and CNES real-time products. More interestingly, the precision of the BDS-3 satellite's clock from PPP-B2b outperforms that of BDS-3 satellites from CNES, which may benefit the additional ISL observations. The average accuracies of the BDS-3 clock from PPP-B2b and CNES are 0.12 ns and 0.23 ns, respectively.

Experimental setup

To test and investigate the performance of real-time PPP time transfer with the PPP-B2b service, detailed information on stations from MGEX is introduced in this part. Processing strategies are then illustrated in detail.

Dataset

Since there are not many GNSS stations connected to an atomic clock in the Asia–Pacific region for time transfer, we only chose 2 GNSS stations, namely USUD and CUSV (Fig. 5). USUD is equipped with an H-master clock. Station

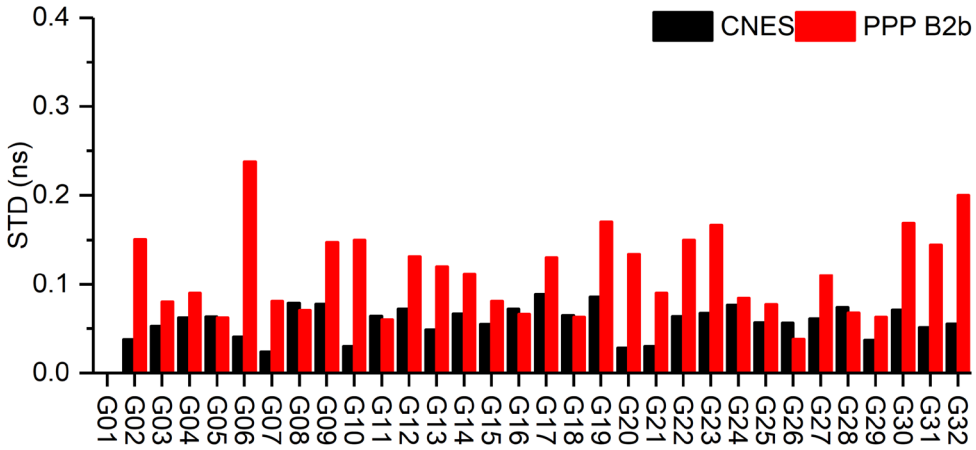

Fig. 3 The STD values of double-difference of GPS satellites clock in the CNES's real-time products and PPP-B2b

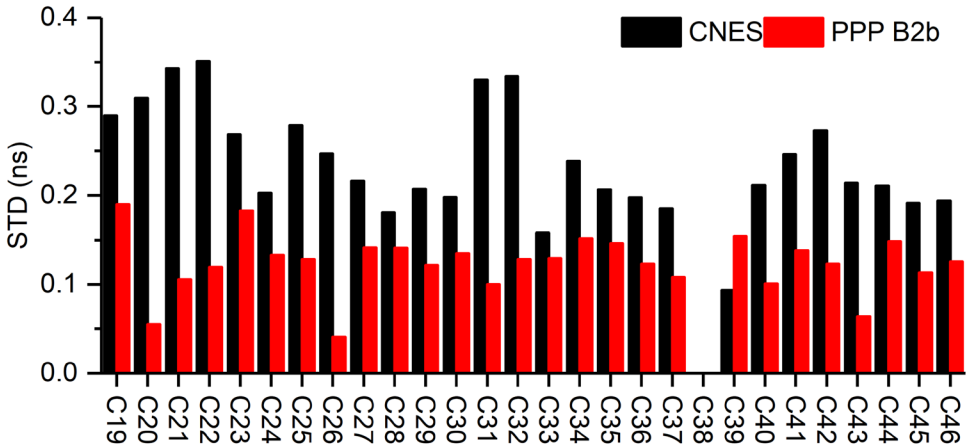

Fig. 4 The STD of double-difference of satellites clock for the CNES's real-time products and PPP-B2b

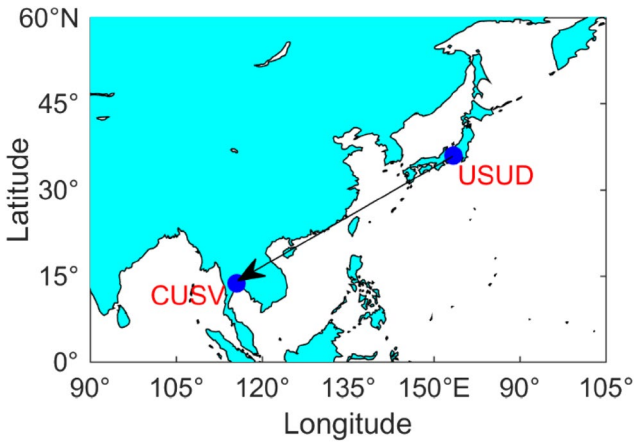

Fig. 5 Selected stations for time transfer from MGEX. Both stations are located in the Asia Pacific region and the PPP-B2B service can cover both regions. CUSV and USUD stations are equipped with high-performance crystal and hydrogen clocks, respectively

CUSV does not link atomic clocks, but its frequency source is relatively stable, so we also chose it for experiments. The observations cover 29 days from DOY 122 to 131, 2022, and from DOY 144 to 162, 2022. Note that data from DOY 132 to 143, 2022 were an internet interruption. The precise products will be recovered with LANV and CNAV1 broadcast ephemeris and the PPP-B2b correction. The CNES real-time products were received and recovered by BNC software (Weber et al. 2016). Final products and ultra-rapid products released from Wuhan university were downloaded from ftp://igs.gnsswhu.cn/. Note that ultra-rapid products were called WUU for ease of expression in this work.

Processing strategy

In our work, the strategies of PPP time transfer are summarized in Table 2. Those known errors, such as relativistic effects, Sagnac effect et al., are modified by the IERS standard models (Petit and Luzum 2010). The receiver clock offset was regarded as white noise to estimate. BDS-3, GPS, and BDS-3/GPS PPP time transfer with the PPP-B2b were designed and compared with PPP with CNES, WUU, and WUM products. Here, the time transfer solutions from the IGS final clock products were set as the time standard. Note that considering the convergence of the PPP time transfer, the results of the first day were not used for the calculation of

Table 2 Summary of PPP time transfer as used in this contribution

Estimator	Kalman filter
Signals	BDS-3: B1I/B3I GPS: L1/L2
PCV and PCO	igs14.atx
Receiver clock offset	Estimated with a white noise model (10^4 m^2)
Precise products	Broadcast ephemeris (CNAV1 or LNAV) + PPP-B2b correction
	Broadcast ephemeris + CNES's real-time correction
	WUM final products
Tropospheric delay	ZHD: corrected (Saastamoinen 1972)
	ZWD: estimated with a random walk noise model (3×10^{-8} m^2/s)
Tidal displacement	Corrected (Petit and Luzum 2010)
Phase ambiguities	Estimate as constant at each arc; When cycle-slip happened, estimated as white noise model (10^4 m^2)
Receiver coordinates	Estimate as constant

the precision. In addition, for the BDS-3/GPS PPP model, an inter-system bias (ISB) parameter will be added. Here, the receiver clock offset was set to BDS-3 observations, while the receiver clock offset of GPS observations will consist of the receiver clock offset of BDS-3 and ISB. Note that a backward filter was not employed in this study. In addition, MEO and GEO weighting ratio is 10:1 for BDS-3 PPP processing.

Results and validation

The time transfer based on PPP using the PPP-B2b service was investigated and compared with PPP using WUM, WUU, and CNES products. The STD values of the difference between time transfer solutions and the reference were employed to reflect the noise level. In addition, the MDEV was also utilized to assess real-time PPP in the frequency domain. Note that the CNES products in the full text represent the CNES real-time products. Below B2b indicates the real-time products recovered from the PPP-B2b correction. Note that B2b indicates the PPP-B2b in this contribution.

Before studying time transfer, we give the number of satellites involved in PPP with B2b products at two stations and display it in Fig. 6. The average numbers of satellites involved in PPP are (5.2, 6.9, 11.2) at station USUD and (5.3, 7.5, 12.2) at station CUSV for GPS-only, BDS-3-only, and BDS-3/GPS. The satellite number of BDS-3 is significantly more than GPS. In addition, we can see that there are some epochs where the number of used GPS satellites is under 3 in the PPP processing, which is similar to BDS-3 satellites. That can be explained by two facts. The one fact is that, unlike final precise products, the PPP-B2b service does not provide all GPS or BDS-3 satellite orbit and clock corrections at any given moment. The other fact is that some

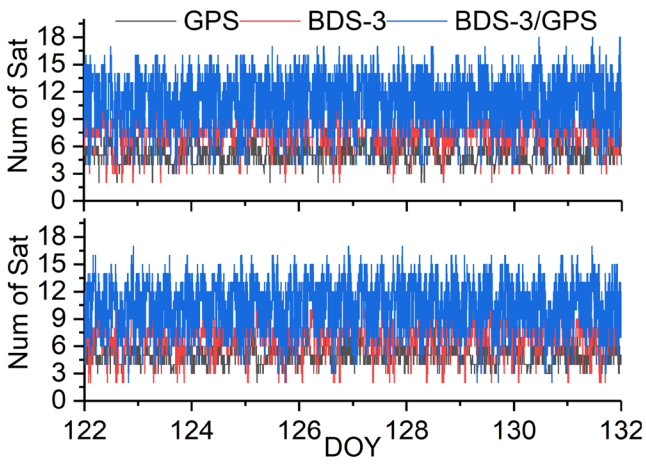

Fig. 6 Number of satellites for BDS-3, GPS, and BDS-3/GPS used in PPP with the PPP-B2b service

satellites have been removed due to their large residuals. After the filter update, we check the observation residuals for each satellite. If the residual of the certain satellite exceeds, the weight of this abnormal observation is reduced, and restart the filter. If the result is still not qualified, we will further eliminate the satellite with too large residuals.

GPS-only

Now turn to Figs. 7 and 8, which exhibited the receiver clock offset for 29 days at CUSV and USUD stations, respectively. From Fig. 7, the receiver clock offset based on the four products does not coincide very well, which can be further proved in Fig. 8. Especially in Fig. 8, we find that the time series of receiver offset using B2b is disorderly and discontinuous, which is because the reference of GPS in B2b is not the same clock. Further, the reference to GPS in CNES and WUU products is also discontinuous. Besides,

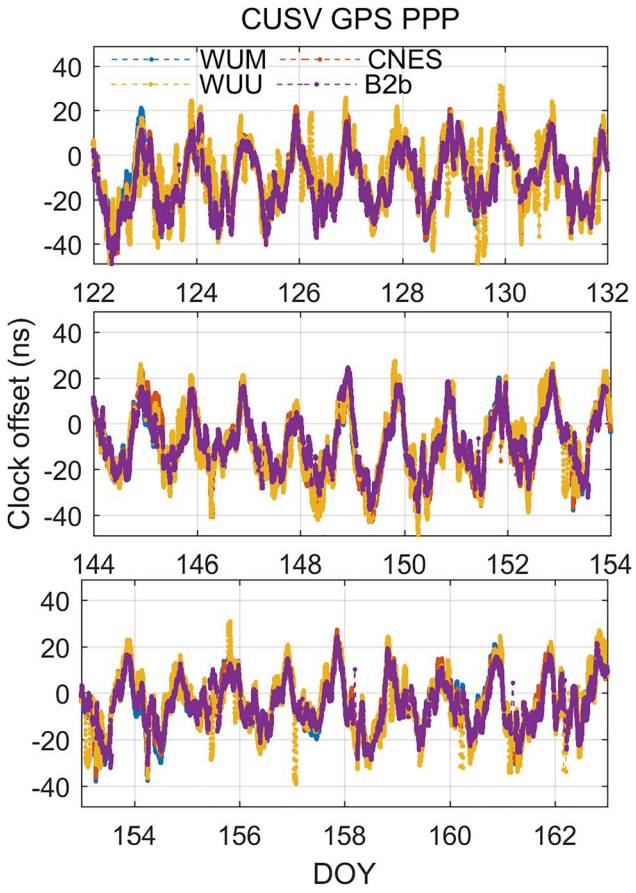

Fig. 7 Receiver clock offset for station CUSV estimated from GPS PPP using WUM, CNES, WUU, and B2b products

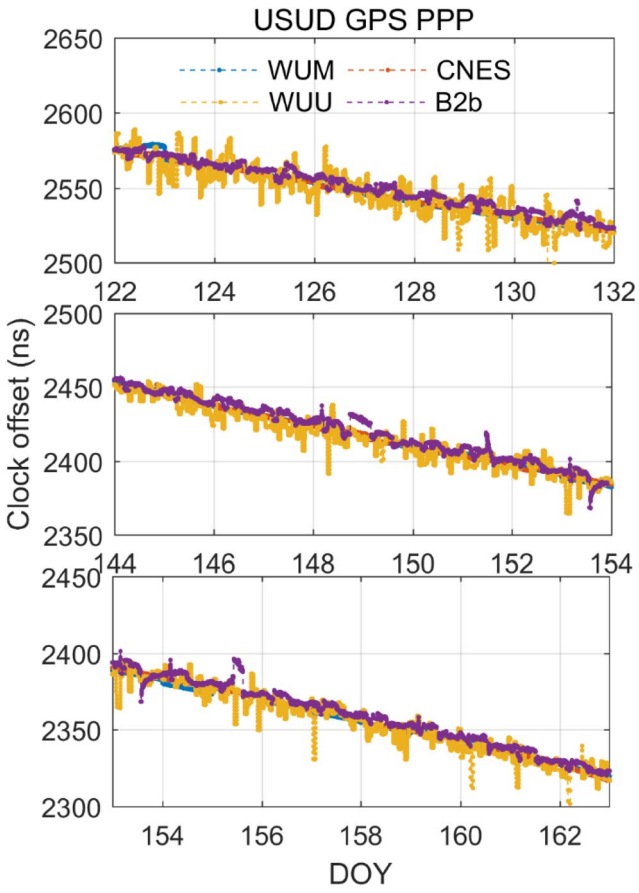

Fig. 8 Receiver clock offset for station USUD estimated from GPS PPP using WUM, CNES, WUU, and B2b products

the noise of the time series obtained from PPP using WUU products is larger because the sampling interval of the WUU products is 5 min. Moreover, the reference of the GPS clock in WUM products is continuous for one day and discontinuous between different days. Luckily, the performance of time transfer is not affected by the reference of a precise clock product (see Eq. 8). In addition, from the figures, there is an understandable phenomenon that receiver clock offsets

Table 3 Availability percentages for PPP solutions with each precise product (%)

DOY	122–131	144–153	153–162
WUM	100	100	100
WUU	100	100	100
CNES	97.1	95.3	96.5
B2b	99.9	99.4	99.6

calculated from PPP using the CNES real-time products are prone to interruptions due to the instability of the internet. We can further find the phenomenon in Table 3, which exhibits the availability percentages for PPP solutions with each precise product, compared with the theoretical number of epochs. Obviously, the availability percentages for PPP solutions with B2b are better than that of PPP with CNES. Since we are using the server to receive CNES corrections, the availability percentages of PPP with CNES products achieve about 95–97% only when the network is relatively good. But it is difficult to ensure such a good network environment in the actual application process. This also strongly proves that PPP time transfer using B2b is significantly better than the current that of PPP based on IGS RTS products in terms of reliability. Figure 9 exhibits the clock difference of CUSV-USUD estimated from PPP with WUM, WUU, CENS, and B2b products. As we mentioned, the difference in the reference was removed by using (8) for the time

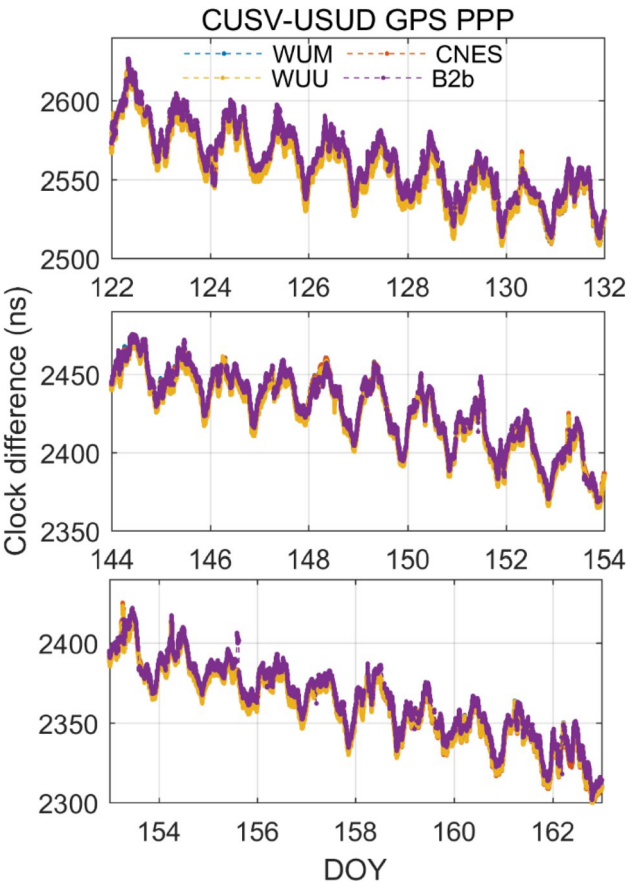

Fig. 9 CUSV-USUD clock difference obtained from GPS PPP using WUM, CNES, WUU, and B2b products

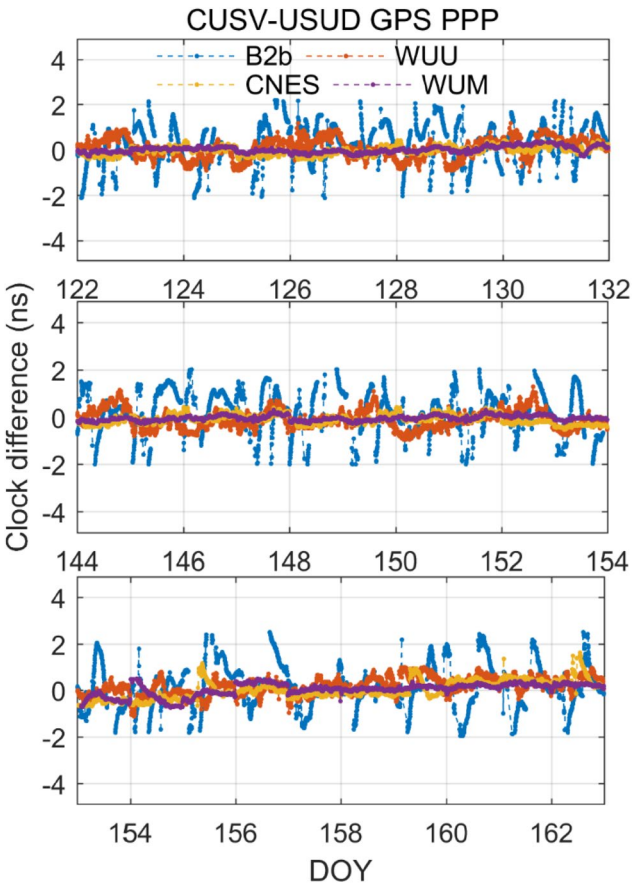

Fig. 10 CUSV-USUD clock difference between GPS PPP using WUM, CNES, and B2b products and the solutions from IGS final clock products

transfer, and the PPP time transfer using different products is generally consistent. Figure 10 displays the clock difference between GPS PPP time transfer with different products and the reference. The performance of GPS PPP with the PPP-B2b is significantly worse than GPS PPP with CNES, WUU, and WUM products. In addition, the STD and mean values of the difference between time transfer solutions and the reference are calculated and listed in Table 4. From the table, two findings are concluded. First, the mean values of time transfer with WUM, WUU, and CNES are close to zero, while that of time transfer with B2b is about 0.5 ns, an obvious system bias. That may be caused by the nonzero mean satellite bias, which has been presented by Tao et al. (2021). Second, the mean STD values of the difference for three arcs obtained from PPP with WUM, CNES, and WUU products are approximately 0.12 ns, 0.23 ns, and 0.50 ns, while that of PPP with B2b products is about 0.89 ns. That may be because GPS orbit and clock precision are poor,

Table 4 Mean and STD of the difference between GPS PPP time transfer using different products and the reference (unit: ns). Note that the time transfer solutions calculated from GPS PPP using IGS final products were set as the time standard

DOY	B2b		WUM		CNES		WUU	
	Mean	STD	Mean	STD	Mean	STD	Mean	STD
122–131	0.55	0.97	0.05	0.13	0.09	0.21	0.08	0.51
144–153	0.53	0.88	0.05	0.15	0.08	0.26	0.09	0.48
153–162	0.58	0.83	0.04	0.10	0.05	0.22	0.06	0.53

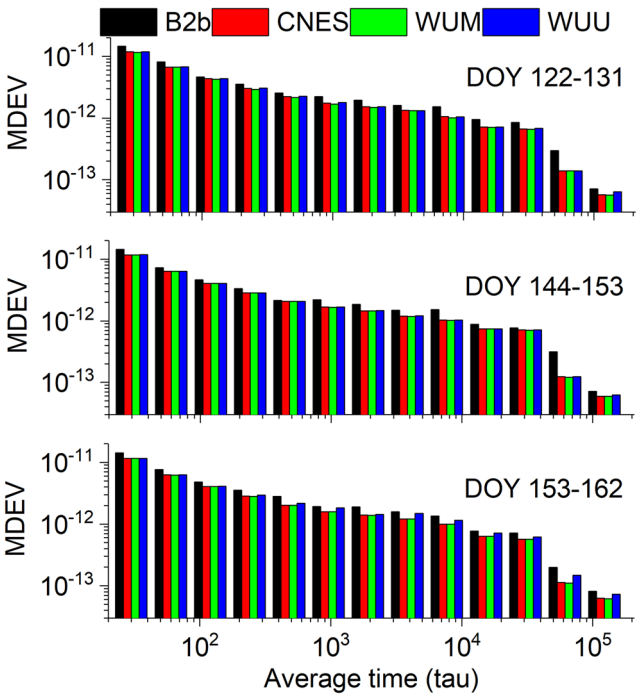

Fig. 11 MDEV of GPS time transfer using WUM, CNES, B2b products

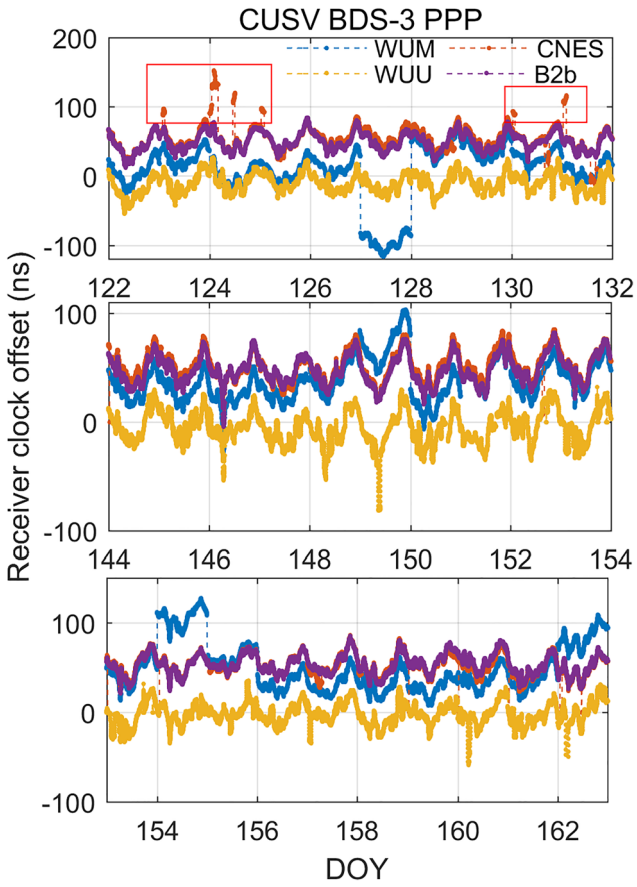

Fig. 12 CUSV receiver clock offset from PPP BDS-3 in WUM, CNES, WUU, and B2b products

and the satellites involved in the time transfer solutions are fewer in the selected station. Combining Tables 3 and 4, PPP time transfer using WUU performs worse than PPP with CNES, but the data integrity of PPP with WUU is better than that of CNES. In addition, let us analyze it further from the frequency domain. Figure 11 presents the MDEV of the solution based on different products. Similarly, the frequency stability of PPP with the PPP-B2b correction presents a worse performance in the four schemes. Hence, the precision of PPP time transfer with CNES products is almost as accurate as that of PPP with WUM products, while that of PPP with the PPP-B2b correction is poor, GPS-only PPP with B2b products is not recommended for time transfer.

BDS-3 only

The receiver clock offset for CUSV and USUD stations estimated from BDS-3 PPP by applying WUM, WUU, CNES, and B2b products are displayed in Figs. 12 and 13. Four interesting findings can be presented. First, unlike GPS PPP with WUM, the jump between days based on

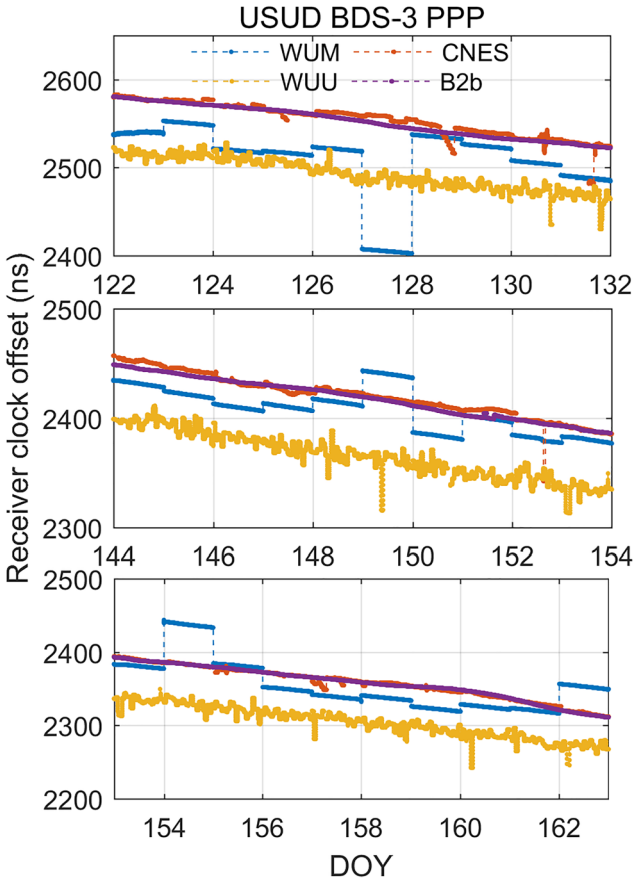

Fig. 13 USUD receiver clock offset from PPP BDS-3 in WUM, CNES, WUU, and B2b products

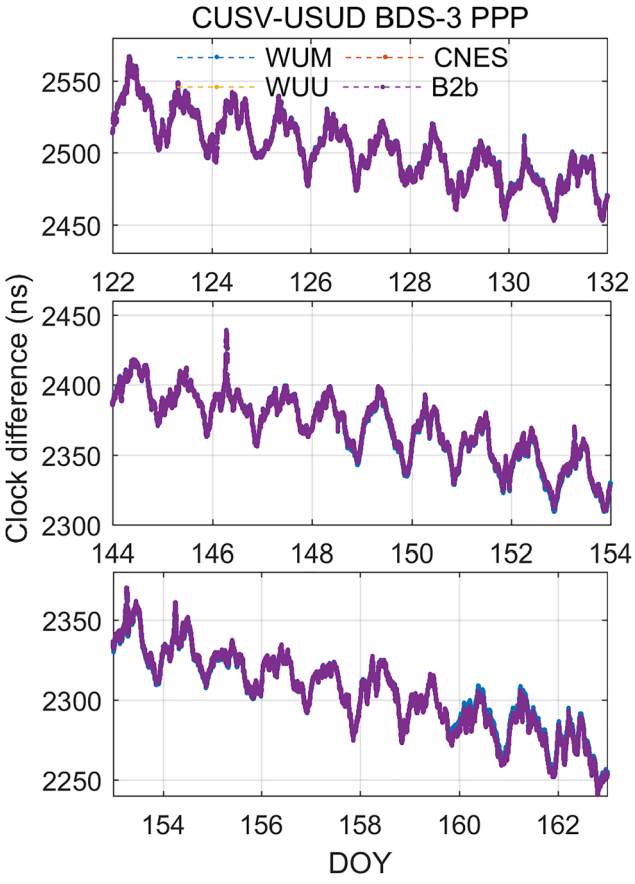

Fig. 14 CUSV-USUD time transfer with BDS-3 PPP using different products

BDS-3 PPP with WUM is very large, but it is still very continuous and stable throughout the day, which is the same as that of GPS PPP. It can be explained by the fact that the reference of GPS and BDS-3 clock in WUM is not the same. Second, although the relative continuity of BDS-3 PPP using CNES is compared to WUM, there are still jumps at the part-time and some outliers. Third, importantly, the BDS-3 PPP with B2b presents a very smooth and continuous time series, it may benefit from the fact the reference of B2b products is BDT. It also releases a signal that PPP based on B2b products can achieve better receiver clock modeling, which also proves from another perspective the superiority of time transfer in the real-time model using BDS-3 in the PPP-B2b. Fourth, the time series of PPP using WUU presents a noticeable jump. That may be because WUU products are updated every hour, so there is a problem of constantly switching between the reference of ultra-rapid products.

The time transfer solutions of CUSV-USUD based on BDS-3 PPP are illustrated in Fig. 14. From the figure, the time series using different products agree well with each other, which indicates the viability of time transfer based on BDS-3 PPP using B2b products. Figure 15 presents the clock difference between BDS-3 PPP time transfer using different products and the reference. Further, the mean and STD values of the difference between BDS-3 PPP using WUM, WUU, CNES, and B2b products and the reference are calculated and introduced in Table 5. The difference in mean values between the four schemes is very small, further proving the feasibility of BDS-3 PPP using B2b numerically. The mean STD values of time transfer are 0.30, 0.14, 0.35, and 0.54 ns for PPP based on BDS-3 with B2b, WUM, CNES, and WUU products. Obviously, the performance of PPP using WUM is best in four schemes, which can be explained because it is, after all, the final product. Another interesting finding is that the performance of time transfer using B2b

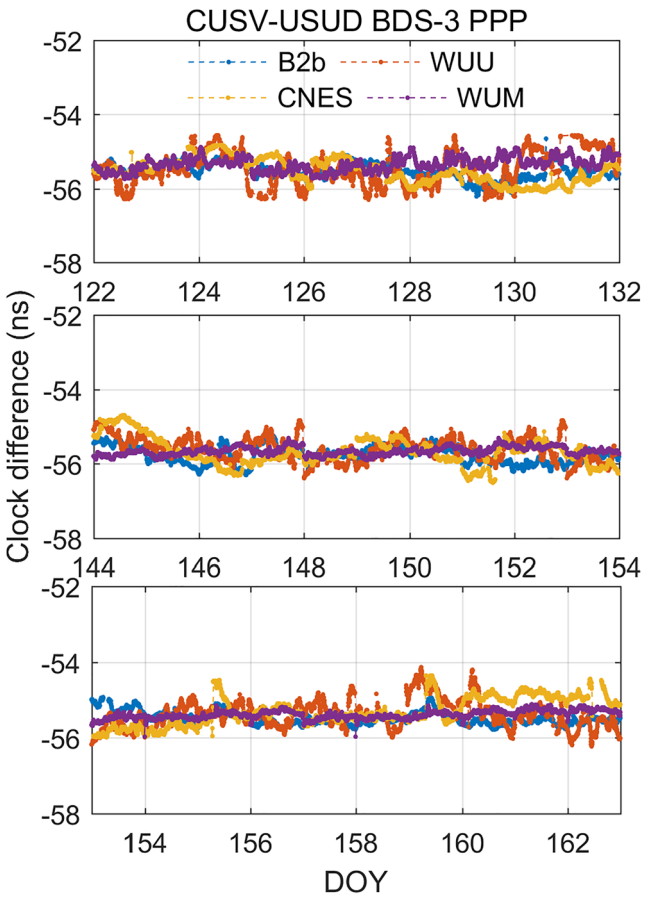

Fig. 15 CUSV-USUD clock difference between time transfer with BDS-3 PPP using different products and time transfer from IGS final products

is slightly better than that of PPP using CNES. That may be because more stations that can track BDS-3 satellites in China were utilized to estimate the satellite orbit and clock, while CNES can use fewer stations in China for satellite clock estimation, and we can further explain the precision of the satellite clock offset (see Fig. 4). The performance of BDS-3 PPP time transfer with WUU products was the worst of the four schemes. In addition, we further calculated the MDEV of BDS-3 PPP using different products and display in Fig. 16. It can be easily found that the frequency stability of PPP using WUM outperforms that of PPP using B2b, and PPP using WUU performs worse. The mean frequency stabilities are about (1.68E-12, 2.00E-12, 1.67E-12, 2.13E-12) at 960 s and about (6.99E-13, 7.39E-13, 6.96E-13, 7.55E-13) at 15,360 s for BDS-3 PPP using B2b, CNES, WUM, and WUU products, which further prove the above finding.

BDS-3/GPS

The characteristic of GPS, BDS-3, and BDS-3/GPS PPP with B2b products is investigated and compared. Figures 17 and 18 display the receiver clock offset for USUD and CUSV stations by using BDS-3, GPS, and BDS-3/GPS PPP. Here, the receiver clock offsets estimated from BDS-3, BDS-3/GPS PPP are basically coincident, while that of GPS PPP presents a large fluctuation, due to the discontinuity of clock reference for GPS in the PP-B2b service. Figure 19 demonstrates the time transfer solutions for CUSV-USUD using GPS, BDS-3, and BDS-3/GPS PPP. In addition, the clock difference between time transfer calculated from GPS, BDSS-3, and BDS-3/GPS PPP with the PPP-B2b and the reference. A systematic bias is found between GPS PPP and BDS-3 PPP or BDS-3/GPS PPP is displayed in Fig. 20. That may be due to the hardware delay at the receiver end. The STD and mean values of the difference between the reference and PPP using B2b products are also listed in Table 6. BDS-3 PPP time transfer precision using B2b product (0.30 ns) is significantly better than GPS PPP (0.89 ns). Compared with BDS-3 PPP, the improvement of precision for BDS-3/GPS PPP is limited by adding GPS observations with 0.28 ns for time transfer. That is because the GPS observation equation has a relatively low weight. After all, the precision of the orbit and clock offset of GPS is lower than that of BDS-3. In addition, the MDEV of BDS-3, GPS, and BDS-3/GPS PPP using B2b products is drawn in Fig. 21. The frequency stability of BDS-3, GPS, and BDS-3/GPS PPP is about (2.11E-12, 1.72E-12, 1.67E-12) at 960 s and

Table 5 Mean and STD values of the time transfer based on BDS-3 PPP using B2b, WUM, and CNES products and the reference (unit: ns)

DOY	B2b		WUM		CNES		WUU	
	Mean	STD	Mean	STD	Mean	STD	Mean	STD
122–131	−55.45	0.28	−55.15	0.14	−55.63	0.31	−54.98	0.49
144–153	−55.73	0.30	−56.86	0.16	−55.02	0.35	−55.30	0.55
153–162	−54.92	0.31	−54.86	0.12	−54.82	0.39	−55.13	0.58

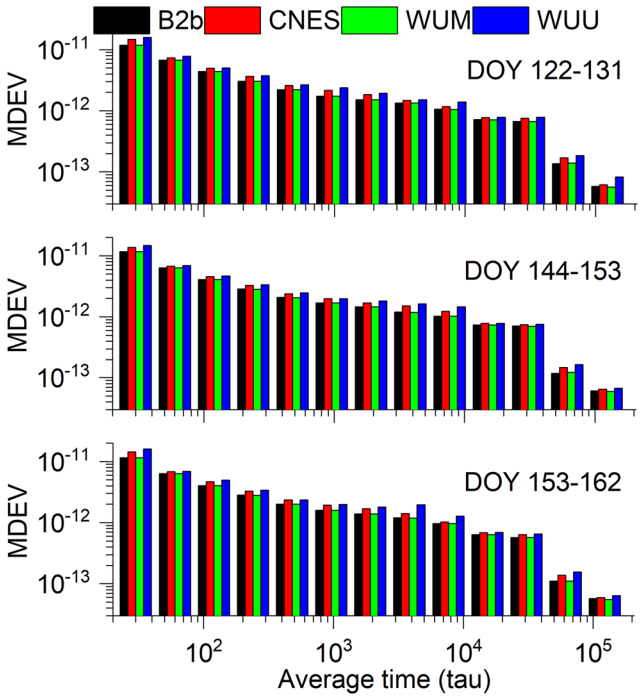

Fig. 16 MDEV of time transfer BDS-3 PPP using different products

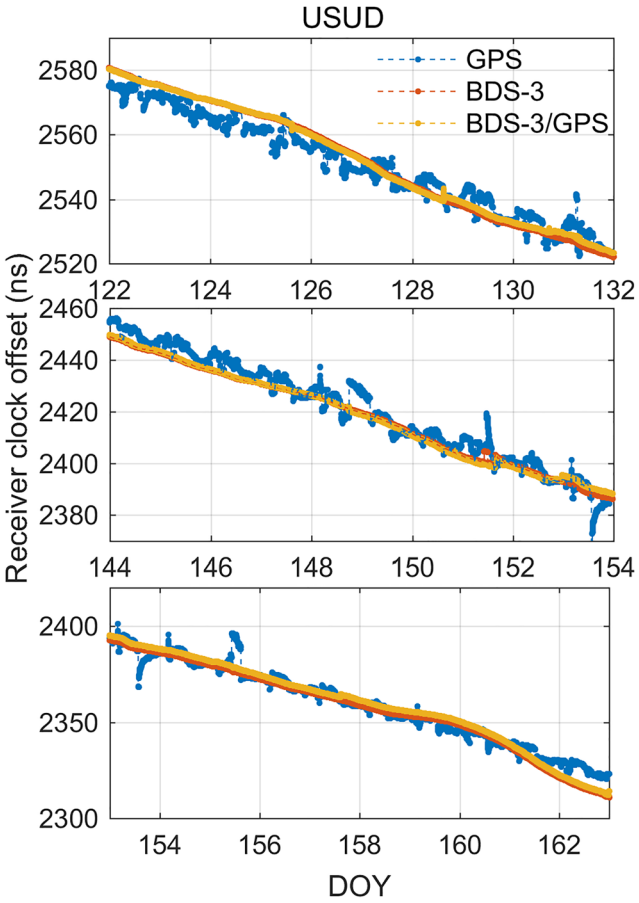

Fig. 17 USUD receiver clock offset from BDS-3, GPS, and BDS-3/GPS PPP using B2b products

about (8.70E-13, 7.02E-13, 6.99E-13) at 15,360 s. The conclusion of frequency stability is similar to the precision of time transfer.

As we mentioned, the convergence time at the beginning of filtering was removed. Here, the mean convergence times for PPP with the PPP-B2b, CNES, WUU, and WUM products at different schemes are calculated and listed in Table 7. We use the positioning error rather than the receiver clock offset time series to calculate the convergence time, which is defined as the time when the horizontal and the vertical positioning error fall within 0.1 m and 0.2 m, respectively. We can find that GPS PPP using the PPP-B2b needs 65.5 min to converge, while the average time for BDS-3 PPP is about 39.5 min. Compared with BDS-3 only, the time of BDS-3/GPS PPP with the PPP-B2b correction can shorten by 16.4%. For PPP with the CNES products, the convergence times for GPS-only and BDS-3-only PPP are 27.5 min and 42 min, respectively. The convergence time of PPP with WUU products is larger than PPP with CENS products, which may be affected by the precision of the satellite clock and the sample interval. In addition, PPP using the WUM products achieved the best results among the three products, with 23.5 min and 26.5 min for GPS-only and BDS-only PPP.

Summary

To meet the requirement of real-time PPP, the PPP-B2b service is provided by BDS-3 for users in China. 29-day PPP-B2b corrections were collected and recovered to the precise product. Then, the BDS-3 and GPS orbit and clock released by CNES and PPP-B2b products were assessed by using WHU final products (WUM) as the reference. The mean RMS of GPS orbit errors is about (0.10, 0.43, 0.23) m and (0.02, 0.03, 0.02) m at RAC direction in PPP-B2b and CNES, respectively. The average RMS values of BDS-3 orbit errors are about (0.07, 0.27, 0.23) m and (0.07, 0.18,

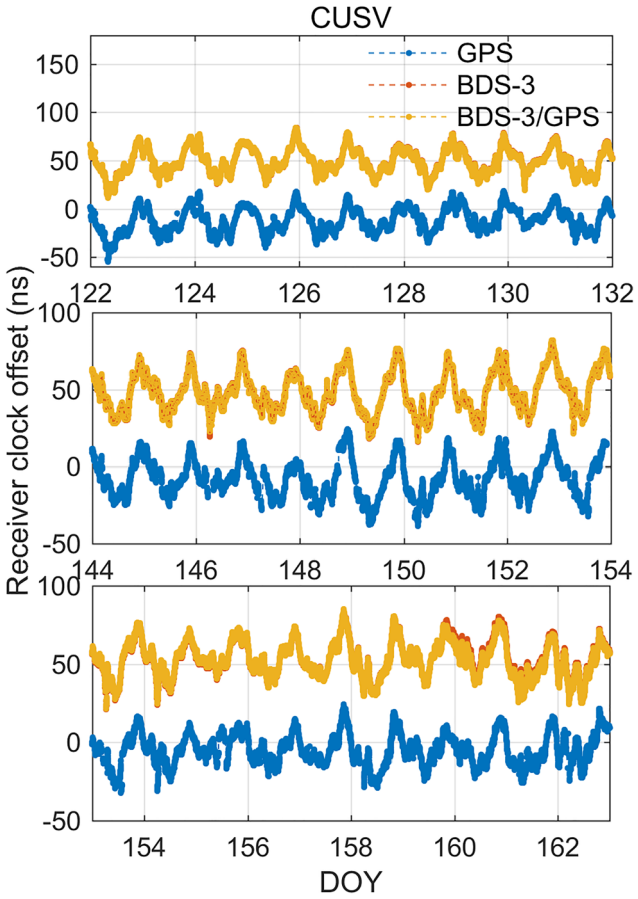

Fig. 18 CUSV receiver clock offset from BDS-3, GPS, and BDS-3/GPS PPP using B2b products

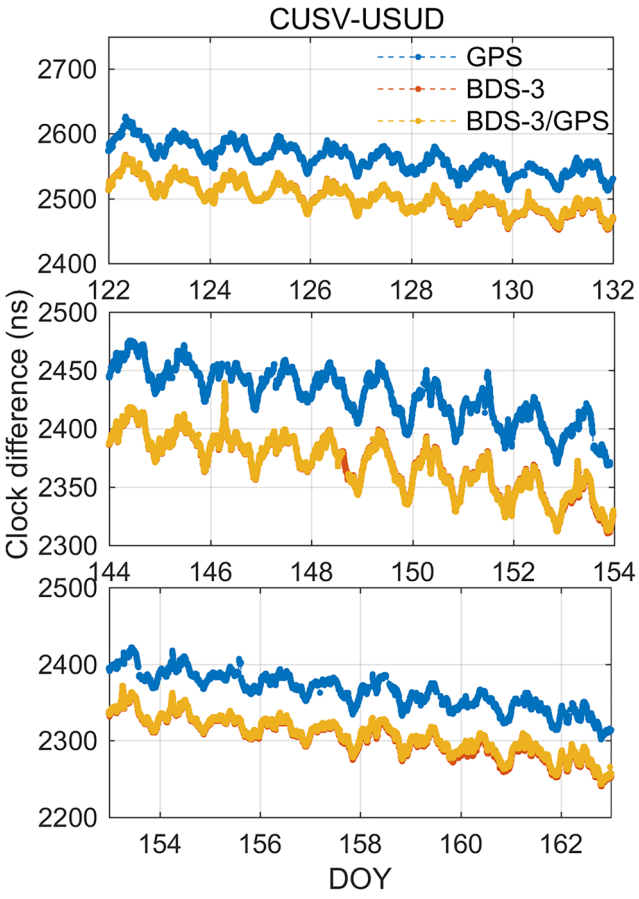

Fig. 19 CUSV-USUD time transfer from BDS-3, GPS, and BDS-3/GPS BDS-3 PPP using B2b products

0.12) m at RAC direction in PPP-B2b and CNES, respectively. In terms of the satellite clock, the STD values of GPS satellites in PPP-B2b are larger than that of CNES. The precision of the BDS-3 satellite clock (0.12 ns) in PPP-B2b outperforms that of BDS-3 satellites in CNES (0.23 ns), due to the additional ISL observations.

The precision of time transfer obtained from GPS PPP using the PPP-B2b products (0.89 ns) is less than that of PPP using the CENS products (0.23 ns). There is a systematic bias between time transfer based on GPS PPP using the PPP-B2b and the time transfer solutions from the IGS final product. Besides, the reference of the satellite clock recovered from PPP-B2b is discontinuous. Overall, we do not recommend time transfer based on GPS PPP with the PPP-B2b service.

The precision of time transfer obtained from BDS-3 PPP using the PPP-B2b, WUM, CENS, and WUU products are 0.30, 0.14, 0.35, and 0.54 ns, respectively. The performance of BDS-3 PPP time transfer using the PPP-B2b products is slightly better than PPP using CNES due to the quality of precise products. Further, the frequency stability of time transfer presents similar conclusions. Hence, the time transfer calculated from BDS-3 PPP with the PPP-B2b is feasible and achieves a good performance. More importantly, real-time BDS-3 PPP using the PPP-B2b products have better reliability because it sometimes does not re-converge due to Internet instability.

Compared with time transfer from BDS-3 PPP using the PPP-B2b, the precision of BDS-3/GPS PPP time transfer was slightly improved. The frequency stability of BDS-3, GPS and BDS-3/GPS PPP are about (2.11E-12,

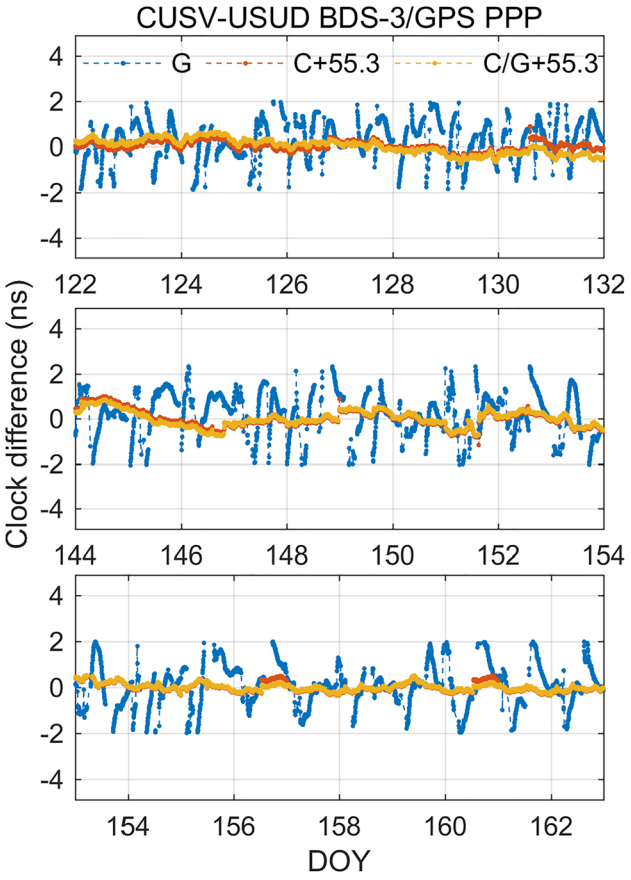

Fig. 20 CUSV-USUD clock difference between time transfer from BDS-3, GPS, and BDS-3/GPS BDS-3 PPP using B2b products and time transfer from IGS final clock products. Note that G and C indicate GPS and BDS-3, respectively

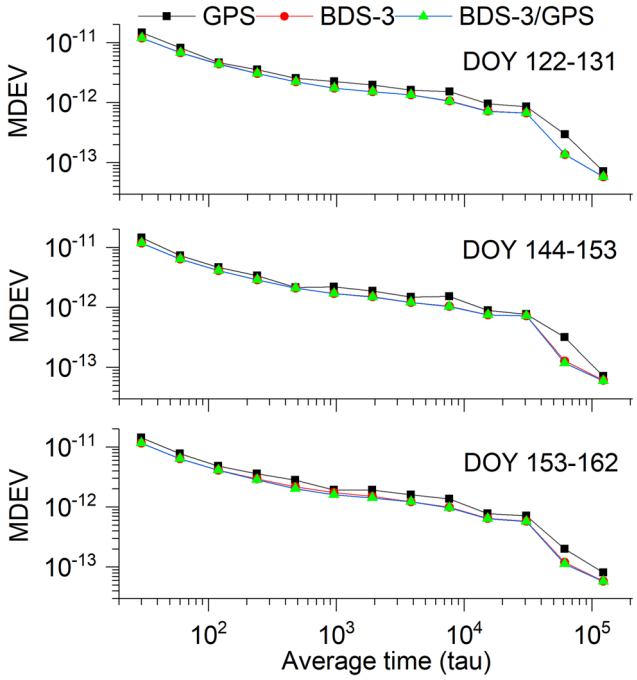

Fig. 21 The MDEV of BDS-3, GPS, BDS-3/GPS PPP using B2b products

1.72E-12, 1.67E-12) at 960 s and about (8.70E-13, 7.02E-13, 6.99E-13) at 15,360 s.

Table 7 The mean convergence time for the two stations with the PPP-B2b, CNES, WUU, and WUM products in static PPP (unit: min)

	GPS	BDS-3	BDS-3/GPS
B2b	65.5	39.5	33.0
CNES	27.5	42.0	26.0
WUM	23.5	26.5	18.5
WUU	56.5	60.0	45.5

Acronyms

APC (Antenna Phase Center), BDS (BeiDou Navigation Satellite System), BDS-3 (Beidou Global Navigation Satellite System), BDT (BeiDou Navigation Satellite System Time), CNES (Centre National d'Etudes Spatiales), DF (Dual-Frequency), DOY (Day of Year), E (East), GNSS (Global Navigation Satellite System), IF (Ionosphere-Free), IFCB (Inter Frequency Code Bias), IGS (International GNSS Service), ISL (Inter-Satellite Link), MGEX (Multi-GNSS Experiment), N (North), OMC (Observed Minus Computed), OSB (Observation-Specific Bias), PCOs (Phase Center Offsets), PCVs (Phase Center Variations), PNT (Positioning, Navigation, and Timing), PPP (Precise Point Positioning), QF (Quad Frequency), RAC

Table 6 STD and mean of BDS-3, GPS, BDS-3/GPS PPP time transfer using B2b products and the reference (unit: ns)

DOY	GPS		BDS-3		BDS-3/GPS	
	Mean	STD	Mean	STD	Mean	STD
122–131	0.55	0.97	−55.45	0.28	−55.41	0.26
144–153	0.53	0.88	−55.73	0.30	−55.62	0.30
153–162	0.58	0.83	−54.92	0.31	−55.39	0.29

(Radial, Along and Cross), RMS (Root Mean Square), RTS (Real-time Service), SF (Single-Frequency), STD (Standard Deviation), TAI (International Atomic Time), TF (Triple-Frequency), URA (User range accuracy), U (Up), ZTD (Zenith Total Delays), ZWD (Zenith Wet Delay).

Acknowledgements We thank MGEX for providing observations. This work was supported by the National Natural Science Foundation of China (No. 42104014; 42077003; 41904018). Natural Science Foundation of Jiangsu Province (No. BK20201374; BK20190714), Natural Science Foundation of the Higher Education Institutions of Jiangsu Province, China (21KJB420005), State Key Laboratory of Geodesy and Earth's Dynamics (SKLGED2022-3-6, SKLGED2022-3-3) and High-level innovation and entrepreneurship talent plan of Jiangsu Province.

Data availability The GNSS data of MGEX are provided by the IGS and can be downloaded through ftp://igs.gnsswhu.cn.

References

Cao X, Kuang K, Ge Y, Shen F, Zhang S, Li J (2022) An efficient method for undifferenced BDS-2/BDS-3 high-rate clock estimation. GPS Solutions. https://doi.org/10.1007/s10291-022-01252-0

CSNO (2019) Development of the BeiDou navigation satellite system (Version 4.0). http://www.beidou.gov.cn/xt/gfxz/201912/P020191227430565455478.pdf

CSNO (2020a) BeiDou navigation satellite system signal in space interface control document open service signal B2b (Version 1.0)

CSNO (2020b) BeiDou navigation satellite system signal in space interface control document precise point positioning service signal PPP-B2b (Version 1.0).

Duan B, Hugentobler U, Chen J, Selmke I, Wang J (2019) Prediction versus real-time orbit determination for GNSS satellites. GPS Solut. https://doi.org/10.1007/s10291-019-0834-2

Ge Y, Cao X, Shen F, Yang X, Wang S (2021a) BDS-3/Galileo time and frequency transfer with quad-frequency precise point positioning. Remote Sens. https://doi.org/10.3390/rs13142704

Ge Y, Chen S, Wu T, Fan C, Qin W, Zhou F, Yang X (2021b) An analysis of BDS-3 real-time PPP: Time transfer, positioning, and tropospheric delay retrieval. Measurement. https://doi.org/10.1016/j.measurement.2020.108871

Guang W, Zhang J, Yuan H, Wu W, Dong S (2020) Analysis on the time transfer performance of BDS-3 signals. Metrologia. https://doi.org/10.1088/1681-7575/abbcc1

Jiao G, Song S, Liu Y, Su K, Cheng N, Wang S (2020) Analysis and assessment of BDS-2 and BDS-3 broadcast ephemeris: accuracy, the datum of broadcast clocks and its impact on single point positioning. Remote Sens. https://doi.org/10.3390/rs12132081

Li G, Lin Y, Shi F, Liu J, Yang Y, Shi J (2018a) Using IGS RTS products for real-time subnanosecond level time transfer. China Satell Navig Conf (CSNC) 497:505–518. https://doi.org/10.1007/978-981-13-0005-9_40

Li X, Chen X, Ge M, Schuh H (2018b) Improving multi-GNSS ultra-rapid orbit determination for real-time precise point positioning. J Geodesy. https://doi.org/10.1007/s00190-018-1138-y

Li X, Yuan Y, Zhu Y, Huang J, Wu J, Xiong Y, Zhang X, Li X (2018c) Precise orbit determination for BDS3 experimental satellites using iGMAS and MGEX tracking networks. J Geodesy. https://doi.org/10.1007/s00190-018-1144-0

Li Z, Chen W, Ruan R, Liu X (2020) Evaluation of PPP-RTK based on BDS-3/BDS-2/GPS observations: a case study in Europe. GPS Solut. https://doi.org/10.1007/s10291-019-0948-6

Liu Y, Yang C, Zhang M (2022) Comprehensive analyses of PPP-B2b performance in china and surrounding areas. Remote Sens. https://doi.org/10.3390/rs14030643

Lu J, Guo X, Su C (2020) Global capabilities of BeiDou navigation satellite system. Satell Navig. https://doi.org/10.1186/s43020-020-00025-9

Malys S, Jensen PA (1990) Geodetic point positioning with GPS carrier beat phase data from the CASA UNO experiment. Geophys Res Lett 17(5):651–654

Montenbruck O, Steigenberger P, Hauschild A (2014) Broadcast versus precise ephemerides: a multi-GNSS perspective. GPS Solut 19(2):321–333. https://doi.org/10.1007/s10291-014-0390-8

Montenbruck O, Steigenberger P, Prange L, Deng Z, Zhao Q, Perosanz F, Romero I, Noll C, Stürze A, Weber G, Schmid R, MacLeod K, Schaer S (2017) The Multi-GNSS experiment (MGEX) of the international GNSS service (IGS)–achievements, prospects and challenges. Adv Space Res 59(7):1671–1697. https://doi.org/10.1016/j.asr.2017.01.011

Petit G, Luzum BJITN (2010) IERS Conventions (2010). 36

Saastamoinen J (1972) Atmospheric correction for the troposphere and stratosphere in radio ranging satellites. Artif Satell Geodesy 15:247–251. https://doi.org/10.1029/GM015p0247

Shi J, Ouyang C, Huang Y, Peng W (2020) Assessment of BDS-3 global positioning service: ephemeris, SPP, PPP, RTK, and new signal. GPS Solut. https://doi.org/10.1007/s10291-020-00995-y

Shi C, Wu X, Zheng F, Wang X, Wang J (2021) Modeling of BDS-2/BDS-3 single-frequency PPP with B1I and B1C signals and positioning performance analysis. Measurement. https://doi.org/10.1016/j.measurement.2021.109355

Tang C, Hu X, Zhou S, Liu L, Pan J, Chen L, Guo R, Zhu L, Hu G, Li X, He F, Chang Z (2018) Initial results of centralized autonomous orbit determination of the new-generation BDS satellites with inter-satellite link measurements. J Geodesy 92(10):1155–1169. https://doi.org/10.1007/s00190-018-1113-7

Tao J, Liu J, Hu Z, Zhao Q, Chen G, Ju B (2021) Initial assessment of the BDS-3 PPP-B2b RTS compared with the CNES RTS. GPS Solut. https://doi.org/10.1007/s10291-021-01168-1

Tu R, Hong J, Zhang P, Zhang R, Fan L, Liu J, Lu X (2019) Multiple GNSS inter-system biases in precise time transfer. Meas Sci Technol. https://doi.org/10.1088/1361-6501/ab32b3o

Wang L, Li Z, Ge M, Neitzel F, Wang X, Yuan H (2019) Investigation of the performance of real-time BDS-only precise point positioning using the IGS real-time service. GPS Solut. https://doi.org/10.1007/s10291-019-0856-9

Weber G, Mervart L, Stürze A, Rülke A, Stcker D (2016) BKG Ntrip Client (BNC) Version 2.12: BKG Ntrip Client (BNC) Version 2.12

Wu Z, Zhou S, Hu X, Liu L, Shuai T, Xie Y, Tang C, Pan J, Zhu L, Chang Z (2018) Performance of the BDS3 experimental satellite passive hydrogen maser. GPS Solut. https://doi.org/10.1007/s10291-018-0706-1

Xiao X, Shen F, Lu X, Shen P, Ge Y (2021) Performance of BDS-2/3, GPS, and galileo time transfer with real-time single-frequency precise point positioning. Remote Sens. https://doi.org/10.3390/rs13214192

Xu Y, Yang Y, Li J (2021) Performance evaluation of BDS-3 PPP-B2b precise point positioning service. GPS Solut. https://doi.org/10.1007/s10291-021-01175-2

Yang Y, Gao W, Guo S, Mao Y, Yang Y (2019) Introduction to BeiDou-3 navigation satellite system. Navigation 66(1):7–18. https://doi.org/10.1002/navi.291

Yang Y, Mao Y, Sun B (2020) Basic performance and future developments of BeiDou global navigation satellite system. Satell Navig. https://doi.org/10.1186/s43020-019-0006-0

Yang Y, Yang Y, Hu X, Tang C, Guo R, Zhou Z, Xu J, Pan J, Su M (2021) BeiDou-3 broadcast clock estimation by integration of observations of regional tracking stations and inter-satellite links. GPS Solut. https://doi.org/10.1007/s10291-020-01067-x

Yang Y, Ding Q, Gao W, Li J, Xu Y, Sun B (2022) Principle and performance of BDSBAS and PPP-B2b of BDS-3. Satell Navig. https://doi.org/10.1186/s43020-022-00066-2

Zeng T, Sui L, Ruan R, Jia X, Feng L (2020) Uncombined precise orbit and clock determination of GPS and BDS-3. Satell Navig. https://doi.org/10.1186/s43020-020-00019-7

Zhang X, Li X, Lu C, Wu M, Pan L (2017a) A comprehensive analysis of satellite-induced code bias for BDS-3 satellites and signals. Adv Space Res. https://doi.org/10.1016/j.asr.2017.11.031

Zhang X, Wu M, Liu W, Li X, Yu S, Lu C, Wickert J (2017b) Initial assessment of the COMPASS/BeiDou-3: new-generation navigation signals. J Geodesy. https://doi.org/10.1007/s00190-017-1020-3

Zhang P, Tu R, Wu W, Liu J, Wang X, Zhang R (2019) Initial accuracy and reliability of current BDS-3 precise positioning, velocity estimation, and time transfer (PVT). Adv Space Res. https://doi.org/10.1016/j.asr.2019.11.006

Zhao X, Ge Y, Ke F, Liu C, Li F (2020) Investigation of real-time kinematic multi-GNSS precise point positioning with the CNES products. Measurement. https://doi.org/10.1016/j.measurement.2020.108231

Zumberge JF, Heflin MB, Jefferson DC, Watkins MM, Webb FH (1997) Precise point positioning for the efficient and robust analysis of GPS data from large networks. J Geophys Res B3(102):5005–5017

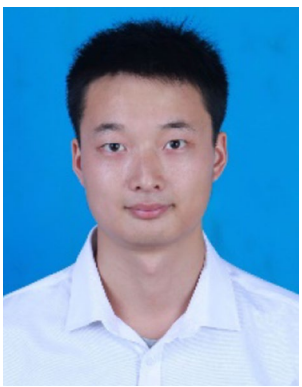

Yulong Ge received his Ph.D. degree from the University of Chinese Academy of Sciences in 2020 and is currently a lecturer at Nanjing Normal University. His current research mainly focuses on high-precise positioning and time transfer using multi-GNSS and multi-frequency PPP.

Xinyun Cao received his Ph.D. degree from Wuhan University in 2018 and is an associate professor at Nanjing Normal University, Nanjing, China. His current research mainly focuses on multi-GNSS high-precise positioning and its geoscience applications.

Daqian Lyu received his Ph.D. degree from the National University of Defense Technology in 2020 and is a lecturer at the National University of Defense Technology. His current research mainly focuses on precise point positioning and time synchronization.

Zaimin He received his Ph.D. from the National Time Service Center (NTSC), Chinese Academy of Sciences (CAS) in 2012 and is now working as a professor and master supervisor at Xi'an University of Posts & Telecommunications. His main research interests are focused on radio positioning, timing, and communication.

Fei Ye received his Ph.D. from the Institute of Geodesy and Geophysics, Chinese Academy of Sciences, in 2019 and is currently a postdoctoral fellow at the Innovation Academy for Precision Measurement Science and Technology, Chinese Academy of Sciences. His research focuses on post- and real-time GNSS precise orbit determination (POD) and Earth rotation parameters (ERP) determination.

Gongwei Xiao received Ph.D. from the State Key Laboratory of Geodesy and Earth Dynamics, Innovation Academy for Precision Measurement Science and Technology, Chinese Academy of Sciences (CAS) in 2021 and is now working as a lecturer with the Xi'an University of Posts and Telecommunications. His current research mainly focuses on multi-GNSS PPP, real-time precise orbit determination for LEO satellites and tropospheric delay. To meet the demands of research and precise point positioning (PPP) in a multi-GNSS environment, he open-sourced a GNSS data processing software named MG-APP (https://geodesy.noaa.gov/gps-toolbox/; https://github.com/xiaogongwei/MG_APP).

Fei Shen received his Ph.D degree from Wuhan University in 2012 and is an professor at Nanjing Normal University, Nanjing, China. His main research interests are interdisciplinary GNSS applications for Earth Observation.